

seems to inhibit angiogenesis in the liver of *Pdgf-c Tg* mice, which might prevent the development of hepatic tumors.

Peretinoin inhibits canonical Wnt/ β -catenin signaling in *Pdgf-c Tg* mice

The activation of the Wnt/ β -catenin signaling pathway is seen in 17% to 40% of patients with primary HCC (23, 24). Moreover, recent reports suggested an interaction between PDGF signaling and Wnt/ β -catenin signaling (25–27). We evaluated Wnt/ β -catenin signaling in *Pdgf-c Tg* mice

and showed by IHC staining that β -catenin was overexpressed in the submembrane at week 48 (Fig. 7A). Peretinoin significantly reduced this expression (Fig. 7A and B), and Western blotting revealed that accumulation of β -catenin in the nuclear fraction of liver tumor tissues was more preferentially repressed by peretinoin than in the cytoplasmic fraction, although expression was repressed in both fractions (Fig. 7C). Wnt ligand (Wnt5a) and frizzled receptor (Fzd1) expression was significantly upregulated in hepatic tumors compared with normal liver (Fig. 7D). These results together suggest that canonical Wnt/ β -catenin

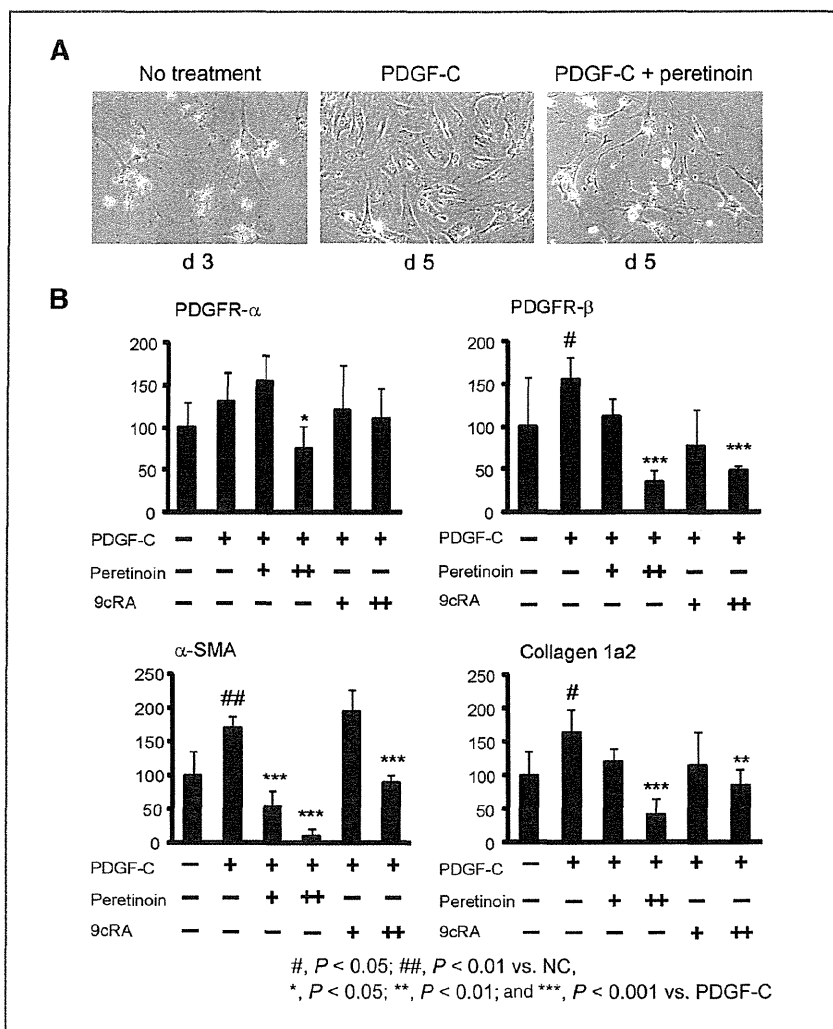


Figure 5. A, microscopic view of freshly isolated primary mouse HSCs after PDGF-C transformation into myofibroblasts (left). Peretinoin inhibited the transformation of HSCs by PDGF-C. B, RTD-PCR analysis of PDGFR- α , PDGFR- β , α -SMA, and collagen 1a2 expression in HSCs treated with or without PDGF-C, peretinoin, and 9cRA ($n = 4$). PDGF-C (+), 80 ng/mL; peretinoin (+), 5 μ mol/L; (++) , 10 μ mol/L; 9cRA (+), 5 μ mol/L; (++) , 10 μ mol/L. NC, no control.

signaling is activated in hepatic tumors and repressed by peretinoin.

Growth factors such as PDGF or HGF potentially activate Wnt/ β -catenin signaling (26, 28), which promotes cancer progression and metastasis. We evaluated whether such growth factor signaling could be repressed by peretinoin in hepatic tumors. The expression of c-myc, β -catenin, Tie2, Fit-1, and Flk-1 were significantly upregulated from 1.5- to 4-fold in hepatic tumors compared with normal liver, and this expression was significantly repressed by peretinoin. Similarly, the expression of PDGFR- α , PDGFR- β , collagen 1a2, collagen 4a2, tissue inhibitor of metalloproteinase 2 (TIMP2), and cyclin D1 was substantially upregulated from 5- to 15-fold in hepatic tumors, and significantly repressed by peretinoin (Fig. 7D). Thus, growth factor signaling as well as canonical Wnt/ β -catenin signaling in hepatic tumors seems to be repressed by peretinoin. These results explain

the inhibitory effect of peretinoin in the development of HCC in *Pdgf-c* *Tg* mice.

Discussion

HCC often develops in association with liver cirrhosis and its high recurrence rate leads to poor patient prognosis. Indeed, the 10-year recurrence-free survival rate after liver resection for HCC with curative intent was shown to be only 20% (29). Therefore, there is a pressing need to develop effective preventive therapy for HCC recurrence to improve its prognosis.

Peretinoin, a member of the acyclic retinoid family, is expected to be an effective chemopreventive drug for HCC (11, 12, 30) as shown by a previous phase II/III trial in which 600 mg peretinoin per day in the Child-Pugh A subgroup reduced the risk of HCC recurrence or death by 40% [HR = 0.60 (95% CI, 0.40–0.89); ref. 31]. However, further clinical

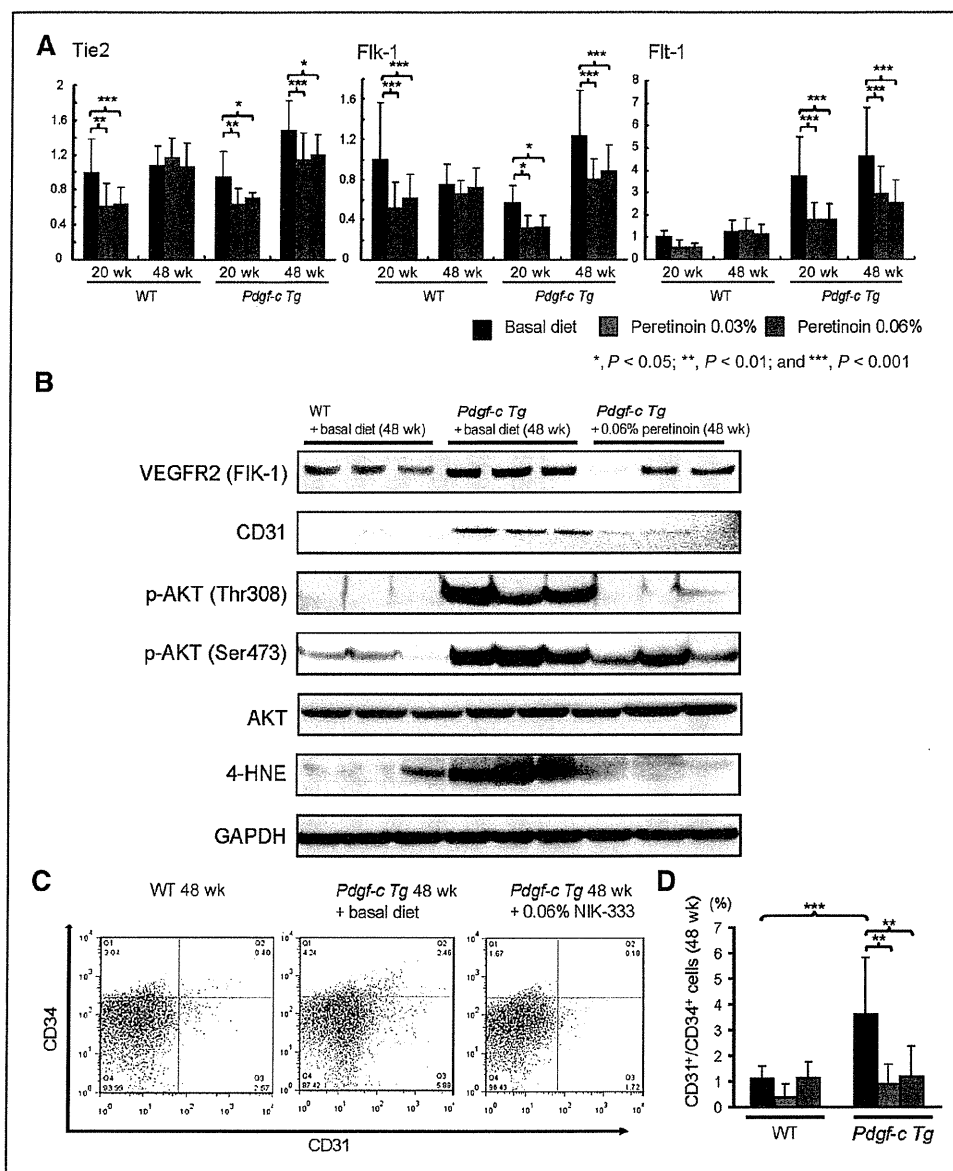


Figure 6. A, RTD-PCR analysis of Tie2, Flk-1, and Flt-1 expression in the liver of *Pdgfr-c Tg* and WT mice fed with different diets (n = 15). B, Western blotting of Flk-1, CD31, p-AKT (Thr 308, Ser473), AKT, 4-HNE, and GAPDH expression in the liver of *Pdgfr-c Tg* or WT mice fed a basal diet or 0.06% peretinoin at 48 weeks (n = 3). C, fluorescence-activated cell-sorting analysis of CD31- and CD34-positive CEC in blood of *Pdgfr-c Tg* or WT mice fed a basal diet or 0.06% peretinoin at 48 weeks. D, frequency of CD31- and CD34-positive CEC in blood of *Pdgfr-c Tg* or WT mice fed a basal diet or 0.06% peretinoin at 48 weeks (n = 10).

studies are needed to confirm the clinical efficacy of peretinoin, and a large scale study involving several countries is currently being planned.

During the course of chronic hepatitis, nonparenchymal cells including Kupffer, endothelial and activated stellate cells release a variety of cytokines and growth factors that might accelerate hepatocarcinogenesis. Although peretinoin has

been shown to suppress the growth of HCC-derived cells by inducing apoptosis and differentiation (32–35), increasing p21 and reducing cyclin D1 (13), limited data have been published about its effects on hepatic mesenchymal cells such as stellate cells and endothelial cells (14).

In parallel with a phase II/III trial, we conducted a pharmacokinetics study of peretinoin focusing on 12

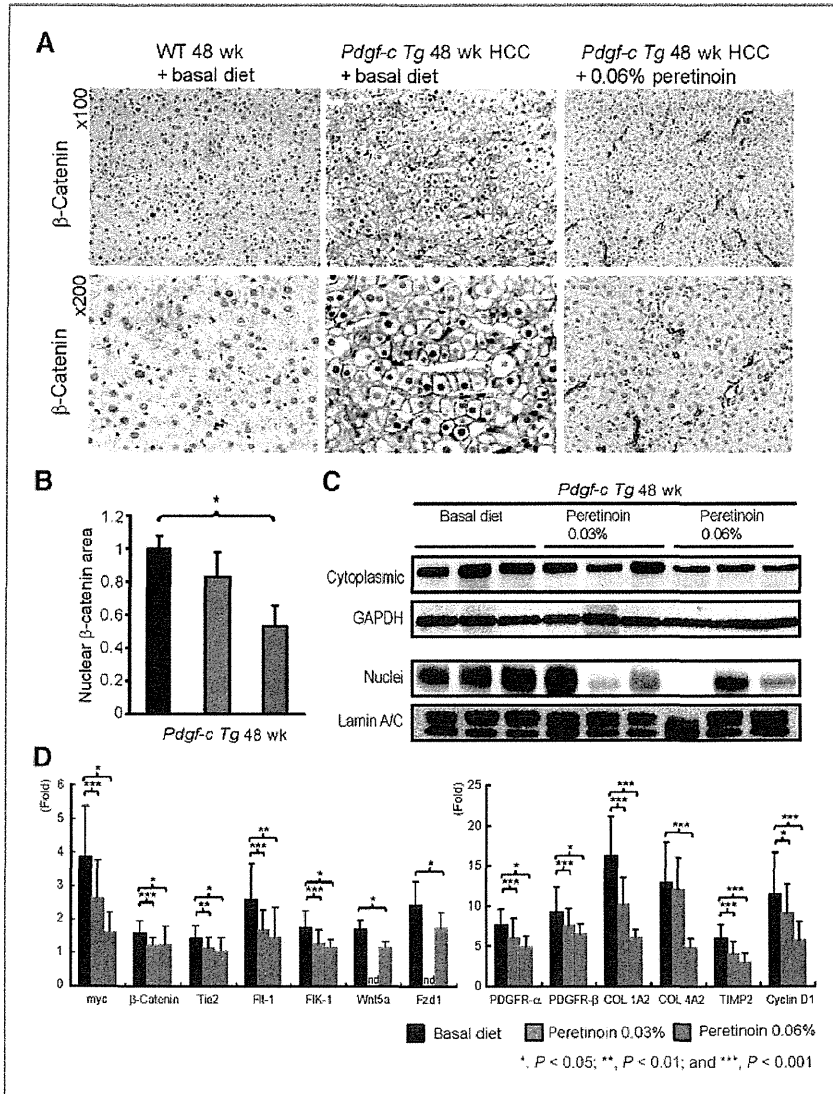


Figure 7. A, IHC staining of β -catenin expression in HCC tissues of *Pdgf-c Tg* mice fed a basal diet or 0.06% peretinoin at 48 weeks. B, densitometric analysis of β -catenin expression in the liver of *Pdgf-c Tg* mice fed with different diets ($n = 15$ for basal diet, $n = 15$ for 0.03% peretinoin, $n = 5$ for 0.06% peretinoin). C, Western blotting of β -catenin expression in cytoplasmic and nuclear fractions of *Pdgf-c Tg* mouse livers fed with different diets. GAPDH was used to standardize cytoplasmic protein and lamin A/C to standardize nuclear protein ($n = 3$). D, RTD-PCR analysis of *myc*, β -catenin, *Tie2*, *Flt-1*, *Flk-1*, *Wnt5a*, *Fzd1*, *PDGFR- α* , *PDGFR- β* , collagen (COL) 1a2, collagen 4a2, *TIMP2*, and *cyclin D1* expression in HCC tissues of *Pdgf-c Tg* mice fed with different diets ($n = 15$ for basal diet, $n = 15$ for 0.03% peretinoin, $n = 5$ for 0.06% peretinoin). Relative fold expressions compared with WT mice are shown.

patients with CH-C and HCC to monitor the biological behavior of peretinoin in the liver. Gene expression profiling during peretinoin administration revealed that HCC recurrence within 2 years could be predicted and that PDGF-C expression was one of the strongest predictors. In addition, other genes related to angiogenesis, cancer stem cell and tumor progression were downregulated, whereas expression of genes related to hepatocyte differentiation and tumor suppression was upregulated by peretinoin (data not shown). Moreover, a recent report revealed the emerging significance of PDGF-C-mediated angiogenic and tumorigenic properties (7, 8, 36). In this study, we therefore used the mouse model of *Pdgf-c Tg*, which displays the phenotypes of hepatic fibrosis, steatosis, and HCC development

that resemble human HCC arising from chronic hepatitis usually associated with advanced hepatic fibrosis.

We showed that peretinoin effectively inhibits the progression of hepatic fibrosis and tumors in *Pdgf-c Tg* mice (Figs. 1 and 4). Affymetrix gene chips analysis revealed dynamic changes in hepatic gene expression (Supplementary Fig. S3), which were confirmed by IHC staining, RTD-PCR and Western blotting. Pathway analysis of differentially expressed genes suggested that the transcriptional regulators Sp1 and Ap1 are key regulators in the peretinoin inhibition of hepatic fibrosis and tumor development in *Pdgf-c Tg* mice (Supplementary Fig. S5).

We clearly showed that peretinoin inhibited PDGF signaling through the inhibition of PDGFRs (Figs. 2 and 3). In

addition, we showed that PDGFR repression by peretinoin inhibited primary stellate cell activation (Fig. 5). Interestingly, this inhibitory effect was more pronounced than the effects of 9cRA (Fig. 5B). Normal mouse and human hepatocytes neither express PDGF receptors (J.S. Campbell and N. Fausto, unpublished data), nor proliferate in response to treatment with PDGF ligands (7). However, peretinoin inhibited the expression of PDGFRs, collagens, and their downstream signaling molecules in cell lines of hepatoma (Huh-7, HepG2, and HLE), fibroblast (NIH3T3), endothelial cells (HUVEC), and stellate cells (Lx-2; Supplementary Fig. S6). Furthermore, Sp1 but not Ap1, might be involved in the repression of PDGFR- α in Huh-7 cells (Supplementary Fig. 6C). The overexpression of Sp1-activated PDGFR- α promoter activity, whereas siRNA knockdown of Sp1 repressed PDGFR- α promoter activity in Huh-7 cells (data not shown). Therefore, this seems to confirm that Sp1 is involved in the regulation of PDGFR, as reported previously (37, 38), although these findings should be further investigated in different cell lines. A recent report showed the involvement of transglutaminase 2, caspase3, and Sp1 in peretinoin signaling (35).

Peretinoin was shown to inhibit angiogenesis in the liver of *Pdgf-c Tg* mice in this study, as shown by the decreased expression of VEGFR1/2 and Tie 2 (Figs. 2 and 6 and Supplementary Fig. S1). Moreover, peretinoin inhibited the number of CD31⁺ and CD34⁺ endothelial cells (CEC) in the blood and liver (Fig. 6C and D), while also inhibiting the expression of EGFR, c-kit, PDGFRs, and VEGFR1/2 in *Pdgf-c Tg* mice (data not shown). We also showed that peretinoin inhibited the expression of multiple growth factors such as HGF, IGF, VEGF, PDGF, and HDGF, which were upregulated from 3- to 10-fold in *Pdgf-c Tg* mice (Supplementary Fig. S3). These activities collectively might contribute to the antitumor effect of peretinoin in *Pdgf-c Tg* mice. The inhibition of both PDGFRs and VEGFR signaling by peretinoin was previously shown to have a significant effect on tumor growth (36), and we confirmed herein that peretinoin inhibited the expression of VEGFR2 in HUVECs (Supplementary Fig. S6; ref. 39). Finally, we showed that peretinoin inhibited canonical Wnt/ β -catenin signaling by showing the decreased nuclear accumulation of β -catenin (Fig. 7). These data confirm the previous hypothesis of transrepression of the β -catenin promoter by 9cRA *in vitro* (40).

Although we showed that the PDGF signaling pathway is a target of peretinoin for preventing the development of hepatic fibrosis and tumors in mice, retinoid-inducing genes such as G0S2 (41), TGM2 (35), CEBPA (42), ATF, TP53BP, metallothionein 1H (MT1H), MT2A, and hemopexin (HPX) were upregulated in peretinoin-treated mice (data not shown). These canonical retinoid pathways are likely to participate in preventing disease progression in conjunction with anti-PDGF effects.

The precise mechanism of peretinoin toxicity, in which 5% of mice treated with 0.06% peretinoin died after 24 weeks of treatment, is currently under investigation. These mice showed severe osteopenia and we speculate that the toxicity might be caused by retinoid-induced osteopenia, as observed in a hypervitaminosis A rat model (43). However, the toxicity of prolonged treatment with oral retinoids in humans remains controversial (44) and severe osteopenia has so far only been seen in a rodent model.

In summary, we show that peretinoin effectively inhibits hepatic fibrosis and HCC development in *Pdgf-c Tg* mice. Further studies are needed to elucidate the detailed molecular mechanisms of peretinoin action and the effect of peretinoin on PDGF-C in human HCC. The recently developed multi-kinase inhibitor Sorafenib (BAY 43-9006, Nexavar) was shown to improve the prognosis of patients with advanced HCC (45). Promisingly, a phase II/III trial of peretinoin showed it to be safe and well tolerated (46). Therefore, combinatorial therapy that incorporates the use of small molecule inhibitors with peretinoin may be beneficial to some patients. The application of peretinoin during pre- or early-fibrosis stage could be beneficial in preventing the progression of fibrosis and subsequent development of HCC in patients with chronic liver disease.

Disclosure of Potential Conflicts of Interest

No potential conflicts of interest were disclosed.

Authors' Contributions

Conception and design: M. Honda, J.S. Campbell, S. Kaneko

Acquisition of data (provided animals, acquired and managed patients, provided facilities, etc.): H. Okada, M. Honda, J.S. Campbell, Y. Sakai, T. Yamashita, Y. Takebuchi, K. Hada, T. Shirasaki, R. Takabatake, M. Nakamura, H. Sunagozaka, N. Fausto

Analysis and interpretation of data (e.g., statistical analysis, biostatistics, computational analysis): J.S. Campbell, T. Yamashita, H. Sunagozaka, S. Kaneko

Writing, review, and/or revision of the manuscript: H. Okada, M. Honda, J.S. Campbell, N. Fausto, S. Kaneko

Study supervision: J.S. Campbell, S. Kaneko

Pathologic examination and evaluation: T. Tanaka

Acknowledgments

The authors thank Dr. Scott Friedman, Mount Sinai School of Medicine (New York, NY), for providing Lx-2 cell lines and Nami Nishiyama and Masayo Baba for their excellent technical assistance.

Grant Support

This work was funded by NIH grants CA-23226, CA-174131, and CA-127228 (J.S. Campbell and N. Fausto). This work was also supported in part by a grant-in-aid from the Ministry of Health, Labour and Welfare, and KOWA Co., Ltd., Tokyo, Japan (M. Honda and colleagues).

The costs of publication of this article were defrayed in part by the payment of page charges. This article must therefore be hereby marked *advertisement* in accordance with 18 U.S.C. Section 1734 solely to indicate this fact.

Received January 9, 2012; revised April 27, 2012; accepted May 18, 2012; published OnlineFirst May 31, 2012.

References

1. Befeler AS, Di Bisceglie AM. Hepatocellular carcinoma: diagnosis and treatment. *Gastroenterology* 2002;122:1609-19.
2. Mohamed AE, Kew MC, Groeneveld HT. Alcohol consumption as a risk factor for hepatocellular carcinoma in urban southern African blacks. *Int J Cancer* 1992;51:537-41.

3. Tsukuma H, Hiyama T, Tanaka S, Nakao M, Yabuuchi T, Kitamura T, et al. Risk factors for hepatocellular carcinoma among patients with chronic liver disease. *N Engl J Med* 1993; 328:1797-801.
4. Deugnier YM, Charalambous P, Le Quilleuc D, Turlin B, Searle J, Brissot P, et al. Preneoplastic significance of hepatic iron-free foci in genetic hemochromatosis: a study of 185 patients. *Hepatology* 1993;18:1363-9.
5. Yeoman AD, Al-Chalabi T, Karani JB, Quaglia A, Devlin J, Mieli-Vergani G, et al. Evaluation of risk factors in the development of hepatocellular carcinoma in autoimmune hepatitis: implications for follow-up and screening. *Hepatology* 2008;48:863-70.
6. Smedile A, Bugianesi E. Steatosis and hepatocellular carcinoma risk. *Eur Rev Med Pharmacol Sci* 2005;9:291-3.
7. Campbell JS, Hughes SD, Gilbertson DG, Palmer TE, Holdren MS, Haran AC, et al. Platelet-derived growth factor C induces liver fibrosis, steatosis, and hepatocellular carcinoma. *Proc Natl Acad Sci U S A* 2005;102:3389-94.
8. Crawford Y, Kasman I, Yu L, Zhong C, Wu X, Modrusan Z, et al. PDGF-C mediates the angiogenic and tumorigenic properties of fibroblasts associated with tumors refractory to anti-VEGF treatment. *Cancer Cell* 2009;15:21-34.
9. Lau DT, Luxon BA, Xiao SY, Beard MR, Lemon SM. Intrahepatic gene expression profiles and alpha-smooth muscle actin patterns in hepatitis C virus induced fibrosis. *Hepatology* 2005;42: 273-81.
10. Honda M, Yamashita T, Ueda T, Takatori H, Nishino R, Kaneko S. Different signaling pathways in the livers of patients with chronic hepatitis B or chronic hepatitis C. *Hepatology* 2006;44: 1122-38.
11. Muto Y, Moriwaki H, Ninomiya M, Adachi S, Saito A, Takasaki KT, et al. Prevention of second primary tumors by an acyclic retinoid, polypropenoic acid, in patients with hepatocellular carcinoma. *Hepatoma Prevention Study Group. N Engl J Med* 1996;334:1561-7.
12. Muto Y, Moriwaki H, Saito A. Prevention of second primary tumors by an acyclic retinoid in patients with hepatocellular carcinoma. *N Engl J Med* 1999;340:1046-7.
13. Suzui M, Masuda M, Lim JT, Albanese C, Pestell RG, Weinstein IB. Growth inhibition of human hepatoma cells by acyclic retinoid is associated with induction of p21(CIP1) and inhibition of expression of cyclin D1. *Cancer Res* 2002;62:3997-4006.
14. Sano T, Kagawa M, Okuno M, Ishibashi N, Hashimoto M, Yamamoto M, et al. Prevention of rat hepatocarcinogenesis by acyclic retinoid is accompanied by reduction in emergence of both TGF-alpha-expressing oval-like cells and activated hepatic stellate cells. *Nutr Cancer* 2005;51:197-206.
15. Muto Y, Moriwaki H, Omori M. *In vitro* binding affinity of novel synthetic polypropenoids (polypropenoic acids) to cellular retinoid-binding proteins. *Gann* 1981;72:974-7.
16. Yamada Y, Shidoji Y, Fukutomi Y, Ishikawa T, Kaneko T, Nakagama H, et al. Positive and negative regulations of albumin gene expression by retinoids in human hepatoma cell lines. *Mol Carcinog* 1994;10:151-8.
17. Honda M, Sakai A, Yamashita T, Nakamoto Y, Mizukoshi E, Sakai Y, et al. Hepatic ISG expression is associated with genetic variation in interleukin 28B and the outcome of IFN therapy for chronic hepatitis C. *Gastroenterology* 2010;139:499-509.
18. Frith C, Ward J, Turusov V. *Pathology of tumors in laboratory animals*. Vol. 2. Lyon, France: IARC Scientific Publications; 1994. p. 223-70.
19. Thoolen B, Maronpot RR, Harada T, Nyska A, Rousseaux C, Nolte T, et al. Proliferative and nonproliferative lesions of the rat and mouse hepatobiliary system. *Toxicol Pathol* 2010;38: 5S-81S.
20. Honda M, Takehana K, Sakai A, Tagata Y, Shirasaki T, Nishitani S, et al. Malnutrition impairs interferon signaling through mTOR and FoxO pathways in patients with chronic hepatitis C. *Gastroenterology* 2011;141:128-40, 140.e1-2.
21. Frith CH, Ward JM, Turusov VS. *Tumours of the liver*. IARC Sci Publ 1994;111:223-69.
22. Xu L, Hui AY, Albanis E, Arthur MJ, O'Byrne SM, Blaner WS, et al. Human hepatic stellate cell lines, LX-1 and LX-2: new tools for analysis of hepatic fibrosis. *Gut* 2005;54:142-51.
23. Nhieu JT, Renard CA, Wei Y, Cherqui D, Zafrani ES, Buendia MA. Nuclear accumulation of mutated beta-catenin in hepatocellular carcinoma is associated with increased cell proliferation. *Am J Pathol* 1999;155:703-10.
24. Wong CM, Fan ST, Ng IO. beta-Catenin mutation and overexpression in hepatocellular carcinoma: clinicopathologic and prognostic significance. *Cancer* 2001;92:136-45.
25. van Zijl F, Mair M, Csiszar A, Schneller D, Zulehner G, Huber H, et al. Hepatic tumor-stroma crosstalk guides epithelial to mesenchymal transition at the tumor edge. *Oncogene* 2009;28: 4022-33.
26. Fischer AN, Fuchs E, Mikula M, Huber H, Beug H, Mikulits W. PDGF essentially links TGF-beta signaling to nuclear beta-catenin accumulation in hepatocellular carcinoma progression. *Oncogene* 2007;26: 3395-405.
27. Hou X, Kumar A, Lee C, Wang B, Arjunan P, Dong L, et al. PDGF-CC blockade inhibits pathological angiogenesis by acting on multiple cellular and molecular targets. *Proc Natl Acad Sci U S A* 2010;107: 12216-21.
28. Apte U, Zeng G, Muller P, Tan X, Micsenyi A, Cieply B, et al. Activation of Wnt/beta-catenin pathway during hepatocyte growth factor-induced hepatomegaly in mice. *Hepatology* 2006;44:992-1002.
29. Eguchi S, Kanematsu T, Arai S, Omata M, Kudo M, Sakamoto M, et al. Recurrence-free survival more than 10 years after liver resection for hepatocellular carcinoma. *Br J Surg* 2011;98:552-7.
30. Okusaka T, Ueno H, Ikeda M, Morizane C. Phase I and pharmacokinetic clinical trial of oral administration of the acyclic retinoid NIK-333. *Hepatol Res* 2011;41:542-52.
31. Okusaka T, Makuuchi M, Matsui O, Kumada H, Tanaka K, Kaneko S, et al. Clinical benefit of peretinoin for the suppression of hepatocellular carcinoma (HCC) recurrence in patients with Child-Pugh grade A (CP-A) and small tumor: a subgroup analysis in a phase II/III randomized, placebo-controlled trial. *J Clin Oncol* 2011;29 Suppl 4s:165.
32. Araki H, Shidoji Y, Yamada Y, Moriwaki H, Muto Y. Retinoid agonist activities of synthetic geranyl geranoic acid derivatives. *Biochem Biophys Res Commun* 1995;209:66-72.
33. Nakamura N, Shidoji Y, Yamada Y, Hatakeyama H, Moriwaki H, Muto Y. Induction of apoptosis by acyclic retinoid in the human hepatoma-derived cell line, HuH-7. *Biochem Biophys Res Commun* 1995;207: 382-8.
34. Yasuda I, Shiratori Y, Adachi S, Obora A, Takemura M, Okuno M, et al. Acyclic retinoid induces partial differentiation, down-regulates telomerase reverse transcriptase mRNA expression and telomerase activity, and induces apoptosis in human hepatoma-derived cell lines. *J Hepatol* 2002;36:660-71.
35. Tatsukawa H, Sano T, Fukaya Y, Ishibashi N, Watanabe M, Okuno M, et al. Dual induction of caspase 3- and transglutaminase-dependent apoptosis by acyclic retinoid in hepatocellular carcinoma cells. *Mol Cancer* 2011;10:4.
36. Timke C, Zieher H, Roth A, Hauser K, Lipson KE, Weber KJ, et al. Combination of vascular endothelial growth factor receptor/platelet-derived growth factor receptor inhibition markedly improves radiation tumor therapy. *Clin Cancer Res* 2008;14: 2210-9.
37. Molander C, Hackzell A, Ohta M, Izumi H, Funa K. Sp1 is a key regulator of the PDGF beta-receptor transcription. *Mol Biol Rep* 2001;28: 223-33.
38. Bonello MR, Khachigian LM. Fibroblast growth factor-2 represses platelet-derived growth factor receptor-alpha (PDGFR-alpha) transcription via ERK1/2-dependent Sp1 phosphorylation and an atypical cis-acting element in the proximal PDGFR-alpha promoter. *J Biol Chem* 2004;279:2377-82.
39. Komi Y, Sogabe Y, Ishibashi N, Sato Y, Moriwaki H, Shimokado K, et al. Acyclic retinoid inhibits angiogenesis by suppressing the MAPK pathway. *Lab Invest* 2010;90:52-60.

40. Shah S, Hecht A, Pestell R, Byers SW. Trans-repression of beta-catenin activity by nuclear receptors. *J Biol Chem* 2003;278:48137-45.
41. Kitareewan S, Blumen S, Sekula D, Bissonnette RP, Lamph WW, Cui Q, et al. G0S2 is an all-trans-retinoic acid target gene. *Int J Oncol* 2008;33:397-404.
42. Uray IP, Shen Q, Seo HS, Kim H, Lamph WW, Bissonnette RP, et al. Retinoid-induced expression of IGFBP-6 requires RARbeta-dependent permissive cooperation of retinoid receptors and AP-1. *J Biol Chem* 2009;284:345-53.
43. Hough S, Avioli LV, Muir H, Gelderblom D, Jenkins G, Kurasi H, et al. Effects of hypervitaminosis A on the bone and mineral metabolism of the rat. *Endocrinology* 1988;122:2933-9.
44. Ribaya-Mercado JD, Blumberg JB. Vitamin A: is it a risk factor for osteoporosis and bone fracture? *Nutr Rev* 2007;65:425-38.
45. Llovet JM, Ricci S, Mazzaferro V, Hilgard P, Gane E, Blanc JF, et al. Sorafenib in advanced hepatocellular carcinoma. *N Engl J Med* 2008;359:378-90.
46. Okita K, Matsui O, Kumada H, Tanaka K, Kaneko S, Moriwaki H, et al. Effect of peretinoin on recurrence of hepatocellular carcinoma (HCC): results of a phase II/III randomized placebo-controlled trial. *J Clin Oncol* 2010;28 Suppl 15s:4024.

CLINICAL STUDIES

Heterogeneous nuclear ribonucleoprotein A2/B1 in association with hTERT is a potential biomarker for hepatocellular carcinoma

Hideki Mizuno¹, Masao Honda^{1,2}, Takayoshi Shirasaki^{1,2}, Taro Yamashita¹, Tatsuya Yamashita¹, Eishiro Mizukoshi¹ and Shuichi Kaneko¹

1 Department of Gastroenterology, Kanazawa University Graduate School of Medicine, Kanazawa, Japan

2 Department of Advanced Medical technology, Kanazawa University Graduate School of Health Medicine, Kanazawa, Japan

Keywords

HCC – hnRNP A2/B1 – hTERT

Abbreviations

HCC, hepatocellular carcinoma; hnRNP A2/B1, heterogeneous nuclear ribonucleoprotein A2/B1; hTERC, human telomerase RNA component; hTERT, human telomerase reverse transcriptase subunit; TRAP, telomere repeat amplification protocol.

Correspondence

Masao Honda, Department of Gastroenterology, Graduate School of Medicine, Kanazawa University, Takara-machi 13-1, Kanazawa 920-8641, Japan
Tel: +81 76 265 2235
Fax: +81 76 234 4250
e-mail: mhonda@m-kanazawa.jp

Received 31 August 2011

Accepted 2 February 2012

DOI:10.1111/j.1478-3223.2012.02778.x

Abstract

Background: The heterogeneous nature of hepatocellular carcinoma (HCC) and the lack of appropriate biomarkers have hampered patient prognosis and treatment stratification. To identify a new prognostic biomarker that is related to human telomerase reverse transcriptase (hTERT) in HCC, we employed a unique proteomics approach using liquid chromatography-mass spectrometry/mass spectrometry (LC-MS/MS) after gel filtration purification of liver tissue. **Methods:** Protein lysates from HCC and cirrhotic liver tissue were subjected to gel filtration using high performance liquid chromatography. The telomerase complex was identified at a molecular mass of 350 kDa in parallel with telomerase activity. These fractionated lysates of 350 kDa were analyzed by LC-MS/MS. The relation of the identified marker and prognosis was statistically examined in surgically resected HCC patients. **Results:** We identified 24 differentially expressed proteins in HCC. One of these proteins, heterogeneous nuclear ribonucleoprotein A2/B1 (hnRNP A2/B1), was further analyzed by immunoprecipitation assay using tissue and cell line samples and found to interact with hTERT. Moreover small interfering RNA against hnRNP A2/B1 suppressed telomerase activity, and immunohistochemical examination showed that the enhanced nuclear and cytoplasmic hnRNP A2/B1 expression in HCC was significantly associated with histological grade of tumor differentiation and microvascular invasion of HCC. Furthermore, survival analysis of 74 HCC patients who received curative surgical treatment showed that hnRNP A2/B1 expression is an independent prognostic factor for patient survival. **Conclusions:** Heterogeneous nuclear ribonucleoprotein A2/B1, an hTERT-associated protein, is a potential prognostic biomarker for HCC patients and might be a therapeutic target of HCC.

Hepatocellular carcinoma (HCC) has extremely poor prognosis and remains one of the most aggressive human malignancies worldwide(1, 2). The high mortality associated with this disease can be attributed mainly to the inability to diagnose HCC patients at an early stage. Currently, α -fetoprotein (AFP) and protein induced by vitamin K absence or antagonists-II (PIVKA-II) are serologic biomarkers for HCC in clinical practice. However, the sensitivity of these markers is not adequate, and a nonspecific elevation in cirrhotic liver is frequently observed. Furthermore, there is an urgent need to identify additional diagnostic as well as prognostic biomarkers of HCC.

Telomerase is a ribonucleoprotein complex that maintains chromosome stability and cell lifespan by telomere maintenance(3–5). The minimal components of active telomerase include human telomerase reverse transcrip-

tase (hTERT), the catalytic subunit, and its template RNA (hTERC) that encodes the template for synthesizing telomeric DNA(6, 7). Various host factors are associated with telomerase and maintain the homeostasis of telomeres(8). Although direct evaluation of protein expression of hTERT would be clinically useful, measurement of hTERT expression in tissue samples is less sensitive and unreliable due to the limitation of appropriate hTERT antibody(9). It would be ideal if some of the hTERT-associated proteins were closely linked to telomerase activity as this could function as a useful biomarker of tumor growth, invasion, and metastasis of HCC.

The aim of this study was to identify a new prognostic biomarker of HCC which was related to hTERT. By employing a proteomics approach combined with gel-filtration protein purification method, we found that the heterogeneous nuclear ribonucleoprotein (hnRNP)

A2/B1 was associated with hTERT and would be a useful prognostic marker of HCC.

Materials and methods

Tissue collection and preparation

All HCC and adjacent cirrhotic (non-cancerous) liver tissue samples were obtained from 74 patients who underwent surgical resection between 2000 and 2009 at Kanazawa University Hospital, Kanazawa, Japan. Follow-ups were terminated in February, 2011. The median follow-up was 38 months (range, 2–83 months). Follow-up data of clinical, aetiological, histological, imaging (ultrasonography, contrast-enhanced helical computed tomography, and magnetic resonance imaging), and treatment details were collected prospectively and added to a customized database as soon as an event such as surgery, follow-up, or death occurred.

Liver tissue samples were formalin-fixed, paraffin-embedded, and used for immunohistochemistry. Histological characterization of HCC and adjacent cirrhotic liver was performed according to the Classification of the Liver Cancer Study Group of Japan and the method described by Desmet *et al.* (10).

For proteomics analysis, three HCC and adjacent cirrhotic liver tissue samples were snap-frozen and stored in liquid nitrogen until later use in gel filtration. Three patients for proteomics analysis belong to the group of 74 patients who underwent surgical resection and were followed-up. The characteristics of these patients were described previously (patients Nos. 4, 8, and 10). All three were positive for Hepatitis C virus (HCV) antibody, and histological examination of HCC was moderately differentiated in two patients and poorly differentiated in one patient (11).

The study was approved by the appropriate ethics committees and the institutional review boards at Kanazawa University and complied with Good Clinical Practice Guidelines, the Declaration of Helsinki, and local laws and regulations.

Preparation of protein lysates and gel filtration of protein lysates

Hepatocellular carcinoma and adjacent cirrhotic liver tissue (100 mg) were ground into powder, homogenized in CelLyticTM MT (detergent, bicine, and 150 mM NaCl; Sigma-Aldrich, St Louis, MO, USA), and sonicated. Protein lysates from the tissue specimens were independently fractionated on HiLoad 16/60 Superdex 200 pg gel filtration columns using a high-performance liquid chromatography (HPLC) system (GE Healthcare, Buckinghamshire, England, UK), which provides rapid screening, method scouting, method optimization, and scale-up experiments, in CelLyticTM MT (Sigma-Aldrich). The resulting fractions were resolved by sodium dodecyl sulfate polyacrylamide gel

electrophoresis (SDS-PAGE), probed with various antibodies, and used for proteomic study by liquid chromatograph-mass spectrometry/mass spectrometry (LC-MS/MS). The column was calibrated with a high molecular weight calibration kit (HMW Native Marker Kit; GE Healthcare).

Protein identification by mass spectrometry

Protein-fractionated lysates were carbamidomethylated by 6M Urea, 500 mM Tris-HCl, 2.5 mM EDTA, and 250 mM iodoacetamide and digested with 100 ng/μL trypsin. Peptide mixtures were redissolved in 0.5% trifluoroacetic acid (TFA), and 1 μg of the peptide solution was mixed with 1 μL of matrix (4-hydroxy- α -cyanocinnamic acid in 30% ACN, 0.1% TFA) before spotting on a target plate. The digested peptides were analyzed by a Hitachi Liquid Chromatograph Mass Spectrometer coupled to a Q-TOF Mass Spectrometer (NanoFrontier eLD; Hitachi High-Technologies Co. Ltd., Tokyo, Japan). The acquired MS/MS spectra were searched for in Swiss-Prot using the Mascot search engine (Matrix Sciences, London, UK). Search parameters were set as follows: peptide mass tolerance, ± 0.3 Da; MS/MS ion mass tolerance, ± 0.3 Da; and trypsin for the enzyme set. The proteins were identified using a *P* value of ≤ 0.05 and Mascot scores of >35 were considered as promising hits. The mean expression ratio of in HCC to proteins identified in adjacent cirrhotic liver tissue was calculated, and a difference of more than two-fold was used as a filtering criterion.

Immunoprecipitation of protein lysates

The protein lysates were incubated at 4°C for 3 h with 10 μL of GammaBind G resin containing prebound anti-FLAG M2 (Sigma-Aldrich) or anti-hnRNP A2/B1 (Abcam, Cambridge, UK), followed by three washes with CelLyticTM MT (Sigma-Aldrich). These bound proteins were separated by SDS-PAGE and visualized by western blotting.

Plasmid construction

The FLAG-GST retrovirus expression vector pBabe-puro-FLAG-GST was constructed by inserting the *FbaI-XhoI* fragment of FLAG-GST cDNA into the *BamHI-Sall* site of the pBabe-puro vector. The GST cDNA of pBabe-puro-FLAG-GST was replaced by the *EcoRI-Sall* fragment containing hTERT cDNA and resulted in retrovirus delivery vector pBabe-puro-FLAG-hTERT (12).

Mammalian cell lines and retrovirus delivery

Huh7 (human hepatocellular carcinoma cell line) and 293T cells (human kidney cell line) were cultured by standard methods in Dulbecco's modified Eagle's med-

ium (DMEM; Gibco BRL, Gaithersburg, MD, USA) supplemented with 10% fetal bovine serum (FBS) and 1% penicillin/streptomycin. Recombinant retrovirus packaging, infection, and selection of FLAG-hTERT expressing stable transformations of Huh7 cells were performed as described(13).

Preparation of cell lysates and immunoprecipitation

Cells were harvested, washed with phosphate buffered solution (-) and sonicated in CelLytic™ M (SigmaAldrich). Lysates of 5×10^6 cells were diluted 10-fold in CelLytic™ M and incubated at 4°C for 3 h with 10 μ L of GammaBind G resin containing pre-bound anti-FLAG M2 or anti-hnRNP A2/B1, followed by three washes with CelLytic™ M. The bound proteins were separated by SDS-PAGE and visualized by western blotting.

Antibodies and western blot analysis

For western blot analysis, total cell lysates and their fractions from gel filtration were separated by SDS-PAGE and transferred to a nitrocellulose membrane then probed with anti-hTERT (Rockland Inc., Gilbertsville, PA, USA), anti-Hsp90 α / β (Santa Cruz Biotechnology, CA, USA), anti-hnRNP A2/B1 (Abcam), anti-FLAG M2 (Sigma-Aldrich), or anti- β -actin (Sigma-Aldrich) primary antibodies, followed by incubation with horseradish peroxidase conjugated goat anti-mouse immunoglobulin (Ig) G secondary antibody (Amersham Biosciences, Buckinghamshire, England, UK) for anti-Hsp90 α / β , anti-hnRNP A2/B1, anti-FLAG M2, and anti- β -actin antibodies or horseradish peroxidase conjugated goat anti-Rabbit IgG secondary antibody (Thermo Scientific, Rockford, IL, USA) for anti-hTERT antibody. Densitometric analysis was conducted directly on the blotted membrane using a CCD camera (LAS-3000 Mini; Fujifilm, Tokyo, Japan) and Scion Image software.

Small interfering RNA synthesis

Small interfering (si) RNA specific to hnRNP A2/B1 (HNRNPA2B1 siGENOME set) and the siGENOME Controls Basic kit were obtained from Thermo Scientific. To each well of a six-well plate, 2×10^5 Huh7 cells were seeded 12 h before transfection. Transfection was performed using TransMessenger™ Transfection Reagent (Qiagen, West Sussex, UK) according to the manufacturer's protocol. A total of 100 pmol/L of siRNA duplex was used for each transfection.

Real-time quantitative reverse-transcription PCR

Real-time quantitative reverse-transcription polymerase chain reaction (RT-PCR) was performed for hnRNP A2/B1 using the ABI Prism 7900HT Sequence Detection System (Applied Biosystems, San Francisco, CA, USA).

Primers and the TaqMan probe for hnRNP A2/B1 were designed using the primer design software Primer Express™ (Applied Biosystems). The probe was labeled with a reporter fluorescent dye (6-carboxy-fluorescein) at the 5' end and a quencher fluorescent dye (6-carboxy-tetramethyl-rhodamine) at the 3' end. PCR conditions were 1 cycle at 50°C for 2 min and 95°C for 10 min, followed by 40 cycles at 95°C for 15 s and 60°C for 1 min. The level of messenger RNA (mRNA) expression relative to the internal control (β -actin) was calculated.

Telomerase activity assay

Telomerase activity was measured by a PCR-based telomere repeat amplification protocol (TRAP) enzyme-linked immunosorbent assay (ELISA). Telomerase activity was quantitatively measured using a TRAPEZE ELISA telomerase detection kit (MILLIPORE, Billerica, MA, USA) according to the manufacturer's protocol.

Immunohistochemical analysis

Paraffin-embedded sections of tissue blocks were orderly rehydrated to xylene and sequential alcohols, washed, and blocked by incubating slides in 0.6% hydrogen peroxide. The sections were treated with a 1:100 diluted solution of anti-hnRNP A2/B1 antibody for 30 min in a wet incubation box. Detection of the antibody was processed according to the manufacturer's protocol using Envision+ kits (Dako, Carpinteria, CA, USA). Slides were counterstained with hematoxylin for 30 s, dehydrated reversibly using sequential alcohols and xylene, and mounted with a coverslip using Histomount. Photographs for stained tissue section were captured using an Olympus DP70 CCD camera with an Olympus AX80 microscope (Olympus, New York, NY, USA).

Statistical analysis

The student's *t*-test was used to determine the statistical significance of the difference in cell viability between the two groups. The chi-square test was used to evaluate the correlation between clinicopathological characteristics and nuclear and cytoplasmic hnRNP A2/B1 expression. Univariate and multivariate Cox proportional hazards regression analysis was used to evaluate the association of nuclear and cytoplasmic hnRNP A2/B1 expression and clinicopathological parameters with patient outcome. All statistical analysis was performed using SPSS software (SPSS software package; SPSS Inc., Chicago, IL, USA).

Results

Fractionation of protein lysates from hepatocellular carcinoma and cirrhotic liver tissue

Protein lysates from HCC and cirrhotic liver tissue from patients were independently subjected to gel filtration

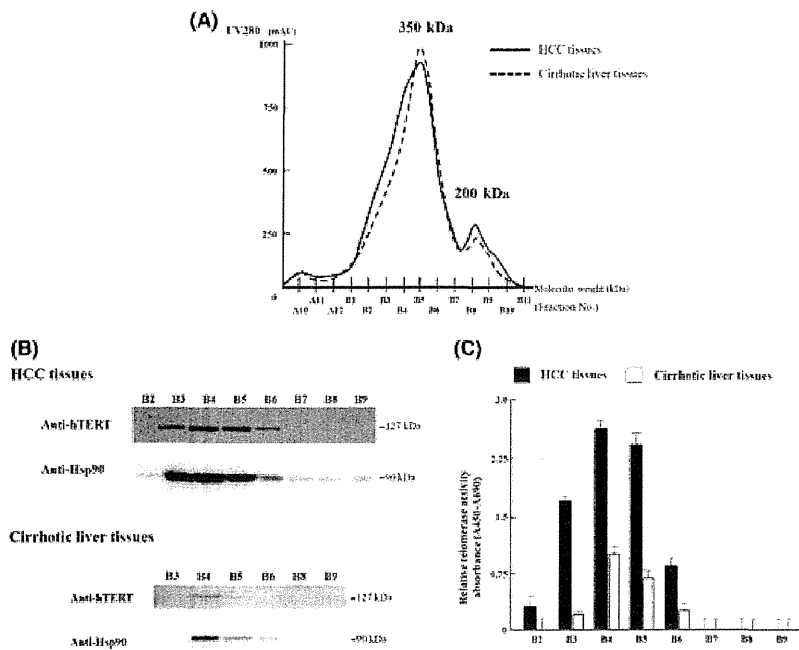


Fig. 1. Fractionation of protein lysates from HCC and cirrhotic liver tissue. (A) Protein lysates from HCC and cirrhotic liver tissues from three patients were fractionated on a 200 μ g gel filtration column by high-performance liquid chromatography (HPLC). Mean values were drawn in the same axis. (B) Representative image of quantitative measurement of human telomerase reverse transcriptase (hTERT) protein and Hsp90 protein by western blotting with respective antibodies. (C) Relative telomerase activity of fractions measured by telomere repeat amplification protocol enzyme-linked immunosorbent assay.

by HPLC (Fig. 1A). Two peaks, corresponding to the molecular weights 350 kDa and 200 kDa in the fractionated proteins were found. Interestingly, hTERT was detected around the 350-kDa peak (Fraction Nos. B3–B6) concurrently with telomerase activity (Fig. 1B, 1C). Moreover Hsp90 was broadly distributed in two peaks of around 350 kDa and 200 kDa (Fraction Nos. B2–B9). The expression of hTERT by western blotting was higher (mean, five-fold) in HCC tissue than that in cirrhotic nodule tissue (Fig. 1B), and the telomerase activity quantified by TRAP ELISA was significantly higher (>2.5-fold) in HCC than in cirrhotic nodule tissue (Fig. 1B, 1C).

Identification of differentially expressed proteins

To discover hTERT-related proteins, we further analyzed the fractionated lysates of the 350-kDa peak (Fraction No. B4) from HCC and cirrhotic liver tissue by LC-MS/MS. After searching the MASCOT database (<http://www.matrixscience.com>), 144 proteins were selected according to identification criteria (see Materials and methods), and 24 of all identified proteins displayed more than a two-fold expression difference. Among these 24 proteins, eight were found to be up-regulated in HCC tissue compared with cirrhotic liver tissue, while 16 proteins were found to be down-regulated (Table 1). Of the 24 proteins, nine were already known

as HCC-related proteins(14–20). To identify a new prognostic biomarker related to hTERT, we decided to focus on hnRNP A2/B1, which has been reported as a prognostic biomarker for lung cancer(21) and gastric cancer(22).

Validation of heterogeneous nuclear ribonucleoprotein A2/B1 expression and interaction with human telomerase reverse transcriptase subunit

To confirm the altered expression of hnRNP A2/B1 in HCC and non-cancerous liver, western blot analysis was performed with anti-hnRNP A2/B1 antibody. Both of hnRNP A2/B1 expression was detected around 350 kDa (Fraction Nos. B3–B7). The hnRNP A2/B1 protein level was higher in HCC tissue than that in non-cancerous liver tissue (Fig. 2A). To examine whether hnRNP A2/B1 can interact with hTERT, we performed an immunoprecipitation assay. hnRNP A2/B1-immunoprecipitates, derived from fractionated lysates of 350 kDa (Fraction No. B4) contained hTERT (Fig. 2B). However, in a reverse immunoprecipitation experiment, anti-hnRNP A2/B1 antibody was unable to recognize the hTERT protein band in hTERT-immunoprecipitates (data not shown). Therefore, we established Huh7 cells derived from stable cell lines that consistently expressed FLAG-tagged hTERT (see Materials and methods). hnRNP A2/B1-immunoprecipitates contained FLAG-hTERT, and

Table 1. Proteins identified by LC-MS/MS as significantly changed in expression between HCC tissues and cirrhotic nodule tissue⁽¹⁸⁻²⁴⁾

Accession no.	Protein name	Molecular function	Protein ratio (HCC/cirrhotic liver)
Up-regulated proteins in HCC tissue			
P 40925	Malate dehydrogenase	L-malate dehydrogenase activity, malic enzyme activity	2.38
Q 13228	Selenium-binding protein 1	Protein binding, selenium binding	2.07
P 22626	Heterogeneous nuclear ribonucleo protein in A2/B1	RNA binding, nucleotide binding	2.01
Q 13535	Serine/threonine-protein kinase ATR	ATP binding, DNA binding	1.92
Q 5T4S7	Zinc finger UBRI-type protein 1	Ubiquitin-protein in ligase activity, zinc ion binding	1.61
P 07335	Annexin A2	Calcium ion binding, cytoskeletal protein binding	1.53
P 30038	Delta-l-pyrroline-5-carboxylate dehydrogenase	1-pyrroline-5-carboxylate dehydrogenase activity	1.52
P 09651	Heterogeneous nuclear ribonucleo protein A1	RNA binding, nucleotide binding	1.48
Down-regulated proteins in HCC tissue			
Q 8NF91	Nesprin-1	Actin binding, lam in binding	0.67
P 00352	Retinal dehydrogenase 1	Ras GTPase activator activity	0.55
P 24752	Acetyl-coA acetyl transferase	Acetyl-coA acetyl transferase activity	0.51
P 00441	Superoxide dismutase (Cu-Zn)	C haperone binding copper ion binding	0.45
P 02787	Serotrnsferin recursor	Ferric ion binding	0.45
Q 8TE73	Ciliaary dyne in heavy chain 5	ATP binding, ATPase activity	0.43
P 07327	Alcohol dehydrogenase 1A	Alcohol dehydrogenase activity (Zinc-dependent)	0.41
P 68871	Hemoglobin subunit beta	Heme binding, hemoglobin binding, oxygen binding	0.39
Q 6PIU 2	Liver carboxyl esterase 1 precursor	Carboxyl esterase activity	0.38
Q 06830	Peroxiredoxin-1	Protein binding, thioredoxin peroxidase activity	0.36
P 69905	Hemoglobin subunit alpha	Heme binding, oxygen binding,	0.34
P 36871	Phosphoglucomutase-1	Magnesium ion binding	0.32
P 05089	Arginase-1	Arginase activity	0.32
P 30041	Peroxiredoxin-6	Glutathione peroxidase activity	0.29
P 00326	Alcohol dehydrogenase 1C	Alcoholdehydrogenase (NAD) activity	0.21
P 08319	Alcohol dehydrogenase 4	NAD binding, NADPH quinone reductase activity	0.15

ATP, adenosine 5'-triphosphate; GTP, guanosine triphosphate; HCC, hepatocellular carcinoma; NAD, nicotinamide adenine dinucleotide; NADPH, nicotinamide adenine dinucleotide phosphate-oxidase.

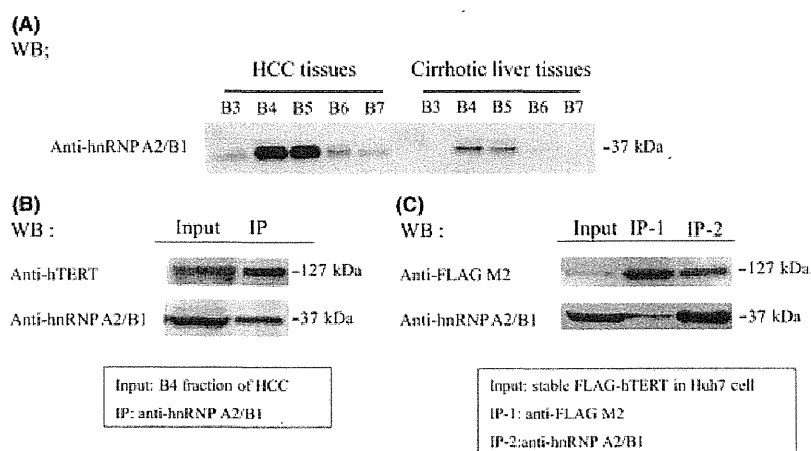


Fig. 2. Validation of hnRNP A1/B2. (A) Representative image of quantitative measurement of hnRNP A2/B1 protein by western blotting with anti-hnRNP A2/B1 antibody. (B) B4 fractionated lysates of HCC were immunoprecipitated with anti-hnRNP A2/B1 antibody. The bound proteins were separated by 8% sodium dodecyl sulfate polyacrylamide gel electrophoresis (SDS-PAGE) and subjected to western blotting with anti-hTERT and anti-hnRNP A2/B1 antibodies as indicated. The B4 fractionated lysates of HCC shown in the input correspond to 5% of the sample. (C) Total cell lysates from Huh7 cells stably expressing FLAG-hTERT were immunoprecipitated with anti-FLAG M2 (IP-1) and anti-hnRNP A2/B1 (IP-2) antibodies. The bound proteins were separated by 8% SDS-PAGE and subjected to western blotting using anti-FLAG M2 and anti-hnRNP A2/B1 antibodies as indicated. Total cell lysates shown in the input correspond to 5% of the sample.

anti-hnRNP A2/B1 antibody recognized the FLAG-hTERT protein band in FLAG-M2 immunoprecipitates (Fig. 2C). These results confirmed that hnRNP A2/B1 can interact with hTERT.

Functional relevance of heterogeneous nuclear ribonucleoprotein A2/B1 expression on telomerase activity

To examine the functional relevance of hnRNP A2/B1 on hTERT activity, we performed knockdown of hnRNP A2/B1. Expression of hnRNP A2/B1 in Huh7 cells was significantly knocked down to 30–40% of the control using hnRNP A2/B1-specific siRNA (siGENOME, Thermo Scientific) (Fig. 3A). Under these conditions, the results of TRAP ELISA showed that telomerase activity was repressed to 43–48% that of the control (Fig. 3B). These results indicate that hnRNP A2/B1 is related to telomerase activity.

Analysis of heterogeneous nuclear ribonucleoprotein A2/B1 expression by immunohistochemistry

To characterize the clinicopathological significance of hnRNP A2/B1 expression in HCC, we performed immunohistochemical staining of hnRNP A2/B1 using paraffin-embedded tumor and non-tumor specimens from 74 HCC patients. We observed hnRNP A2/B1 expression in all HCC specimens, while it was expressed in 16 of 74 (22%) adjacent non-cancerous liver specimens ($P < 0.001$). We did not observe hnRNP A2/B1 expression in normal liver ($n = 5$) or in the early stage (F1–2) of chronic hepatitis ($n = 5$) (data not shown).

Interestingly, we noticed that anti-hnRNP A2/B1 antibody reacted to nuclear and cytoplasmic isoforms of hnRNP A2/B1. We defined HCC cells in which only

nuclear hnRNP A2/B1 was expressed in tumor cells as nuclear hnRNP A2/B1-positive HCC (Fig. 4A). Similarly, both nuclear and cytoplasmic hnRNP A2/B1 was expressed in tumor cells as nuclear and cytoplasmic hnRNP A2/B1-positive HCC, respectively (Fig. 4B). Western blotting analysis showed that hnRNP A2/B1 was expressed significantly more, about 2.5-fold, in the nuclear and cytoplasmic hnRNP A2/B1-positive HCC than in the nuclear hnRNP A2/B1-positive HCC (Fig. 5A, B).

The expression pattern of hnRNP A2/B1 in the nucleus and the cytoplasm was different in each HCC tissue type. Nuclear hnRNP A2/B1-positive HCC was observed in 40.5% (30 of 74) of HCC patients, whereas nuclear and cytoplasmic hnRNP A2/B1-positive HCC was observed in 59.5% (44 of 74) of HCC patients (Table 2). We then compared the clinicopathological features of nuclear hnRNP A2/B1-positive HCC and nuclear and cytoplasmic hnRNP A2/B1-positive HCC (Table 2). Nuclear and cytoplasmic expression of hnRNP A2/B1 was frequently observed in patients with a progressive histological grading (Edmondson-Steiner grades; $P = 0.002$) and microvascular invasion ($P = 0.013$) (Table 2). No relationship was apparent between the expression pattern of hnRNP A2/B1 and age, gender, type of infected virus, Child-Pugh score, AFP value, PIVKA-II value, tumor size, tumor morphology, TNM stages, or recurrence rate of HCC (Table 2). Importantly, survival analysis using the Kaplan-Meier method revealed that HCC patients with nuclear and cytoplasmic expression of hnRNP A2/B1 showed a significant lower survival rate than those with nuclear expression of hnRNP A2/B1 (log-rank test, $P = 0.0027$; Fig. 6). Furthermore, univariate Cox regression analysis showed that nuclear and cytoplasmic expression of hnRNP A2/B1 was significantly associated with low patient survival (HR, 2.37; 95% CI, 1.33–4.23;

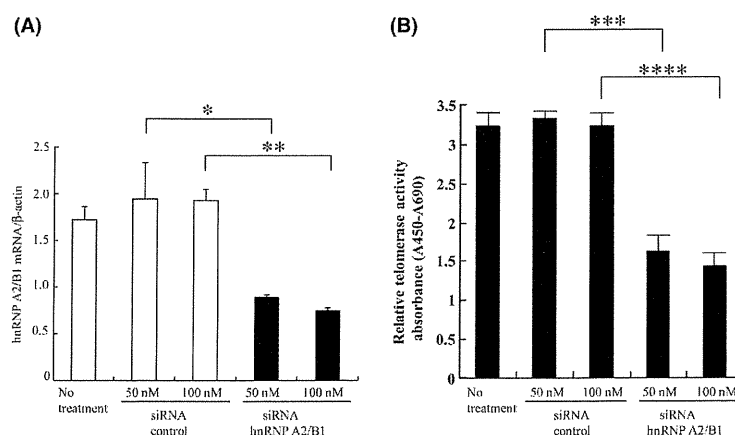


Fig. 3. siRNA against hnRNP A2/B1 suppresses telomerase activity. (A) mRNA expression of hnRNP A2/B1 after small interfering (si)RNA transfection in Huh7 cells transfected with sihnRNP A2/B1 and that of control siRNAs. Levels of mRNA were determined by real time polymerase chain reaction (PCR). (B) The activity of each lysate was determined by TRAP ELISA (*****, $P < 0.05$).

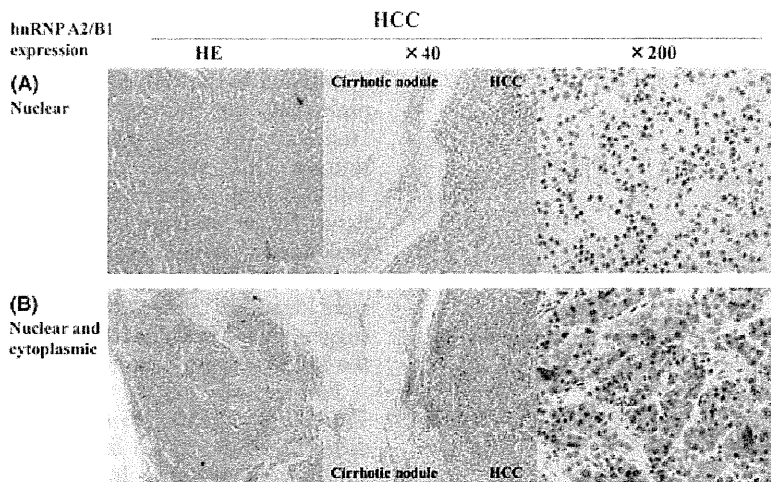


Fig. 4. Immunohistochemical analysis of hnRNP A2/B1 expression in HCC and adjacent cirrhotic liver tissue. A representative photomicrograph of hematoxylin and eosin staining and hnRNP A2/B1 staining in HCC tissue ($\times 40$ and $\times 200$, respectively) and adjacent cirrhotic liver tissue ($\times 40$). (A) Nuclear hnRNP A2/B1-positive HCC. (B) Nuclear and cytoplasmic hnRNP A2/B1-positive HCC.

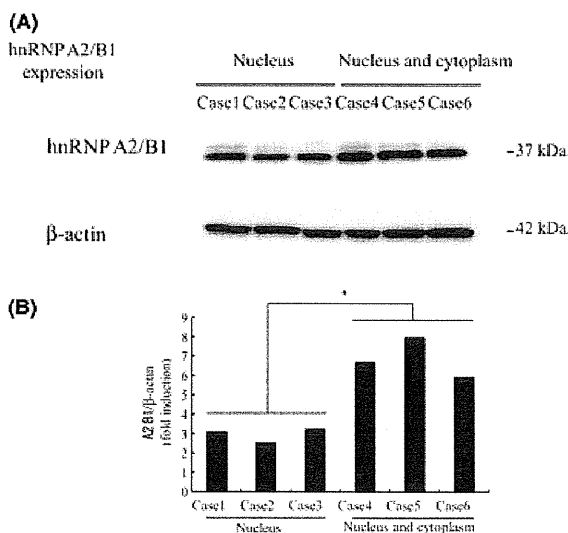


Fig. 5. The protein expression of hnRNP A1/B2 in HCC tissue. (A) Equal amounts of HCC tissue from Nuclear hnRNP A2/B1-positive HCC (cases 1–3) and Nuclear and cytoplasmic hnRNP A2/B1-positive HCC (cases 4–6) were loaded into the SDS-PAGE gel and normalized by comparing with β -actin. (B) The value in the graph is presented as mean \pm SD ($*P < 0.05$).

$P = 0.004$) (Table 3). Multivariate Cox regression analysis showed that nuclear and cytoplasmic expression of hnRNP A2/B1 was an independent prognostic factor associated with low patient survival (HR, 3.86; 95% CI, 1.80–8.28; $P = 0.001$). Other clinicopathological features did not add independent prognostic information in this study (Table 3). These results demonstrate that

Table 2. Clinicopathological characteristics and hnRNP A2/B1 expression of nucleus (&) cytoplasm in HCC ($n = 74$)

	nuclear ($n=30$)	nuclear and cytoplasmic ($n=44$)	P -value
hnRNP A2/B1 expression			
Age (<60 years/ ≥ 60 years)	12/18	18/26	0.938
Gender (male/female)	22/8	18/26	0.531
Virus (HBV/HCV/NBNC)	5/21/4	14/21/9	0.160
Child-Pugh (5/6/7)	28/2/0	37/5/2	0.377
AFP (<100 ng/ml/ ≥ 100 ng/ml)	20/10	26/18	0.509
PIVKA-II (<100 mAU/ml/ ≥ 100 mAU/ml)	18/12	22/22	0.397
Histological grading (well/moderately/poorly)	12/18/0	0/32/12	0.002
Tumor size (<3 cm/ ≥ 3 cm)	16/14	22/22	0.778
Tumor morphology (uni/multi)	26/4	35/9	0.429
TMN classification (VII/III/IVa)	6/17/6/1	2/27/10/5	0.139
Microvascular invasion (Yes/No)	11/19	29/15	0.013
HCC recurrence (Yes/No)	11/19	20/24	0.452

AFP, α -fetoprotein; HBV, Hepatitis B virus; HCC, hepatocellular carcinoma; HCV, Hepatitis C virus.

the expression of hnRNP A2/B1 correlates with the severity and progression of HCC and that nuclear and cytoplasmic hnRNP A2/B1 expression could be a useful biomarker for predicting the survival of HCC patients after surgical resection.

Discussion

The development of useful biomarkers for the early detection and prediction of HCC is urgently required to improve prognosis of patients with HCC. Moreover,

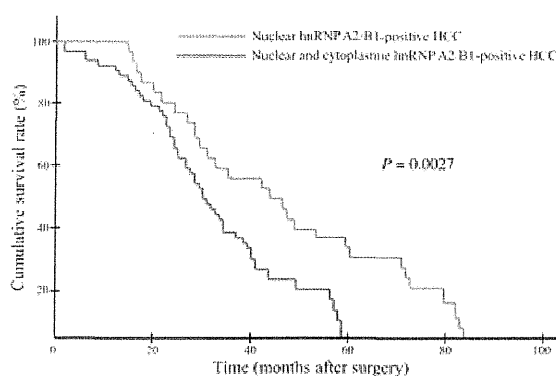


Fig. 6. Kaplan-Meier survival analysis of nuclear (and) cytoplasmic hnRNP A2/B1-positive HCC (log rank test).

biomarkers reflecting malignant features of HCC might be useful for the following patients and HCC therapy selection since HCC relapse frequently occurs in residual liver where HCC has been curatively removed by surgical treatment. Although AFP and PIVKA II are reliable tumor markers for the detection of recurrence of HCC, more than 50% of patients with small HCC (<2 cm) test negative for these markers(23).

A two-dimensional electrophoresis and mass spectrum-based proteomic strategy provide high-throughput simultaneous identification of hundreds of proteins; such a strategy is considered very valuable for screening tumor biomarkers(24, 25). Here, we applied a different approach for identifying telomerase-associated proteins in this study. According to previously reported methods (12), protein lysates of HCC tissue and non-cancerous tissue were subjected to HPLC gel filtration. A previous study using a soluble fraction of Huh7 cells identified two peak of endogenous hTERT at around 680 kDa and 350 kDa (data not shown). It was speculated that a

dimer form of hTERT existed in the 680 kDa peak and a monomer in the 350 kDa peak. Hsp90 was exclusively distributed in the 350 kDa peak but not in the 680 kDa peak (data not shown). Unlike previous studies using Huh7 cells, we could not detect the 680 kDa peak fraction in HCC tissue. We could however detect the 350 kDa peak and the 200 kDa peak fraction in HCC tissue. The telomerase complex existed in the 350 kDa peak fraction. Moreover, Hsp90 existed in 350 kDa peak fraction, while many of the metabolic-related proteins were identified in the 200 kDa peak fraction. These data suggest that hTERT-associated proteins might exist in the 350 kDa peak fraction in HCC tissue.

Further analysis of the fractionated lysates of 350 kDa by LC-MS/MS revealed that 24 proteins were differentially expressed in HCC tissue when compared with nontumor tissue. In addition, 9 of the 24 proteins were already known as HCC-related proteins(14–20). We therefore focused on hnRNP A2/B1, one of the most abundant and important nuclear RNA-binding proteins involved in packaging nascent mRNA, alternative splicing(26, 27) and cytoplasmic RNA trafficking(28), translation(29), and stabilization(30).

To our knowledge, this is the first demonstration of hnRNP A2/B1 interaction with hTERT by immunoprecipitation *in vitro* and *in vivo*. hnRNP A2/B1 acts as a molecular adapter between single-stranded telomeric repeats or telomerase RNA (hTERC), and another segment of single-stranded DNA(31, 32). However the details for such an interaction need further investigation. Of the telomerase-related proteins, Hsp90 has been shown to be a functionally critical factor for telomerase activity *in vivo* and *in vitro*(33). The telomerase complex with Hsp90 within the 350 kDa complex was also detected in this study, confirming the biological functionality of telomerase activity (Fig. 1B,C). Hsp90 inhibitors reduce the amount of hTERT as well as telomerase activity(12). Despite the concentration of Hsp90

Table 3. Cox regression analysis of cumulative survival rate relative to nuclear and cytoplasmic hnRNP A2/B1 expression and clinicopathological parameters of primary HCC patients ($n=74$)

Variables	Univariate		Multivariate	
	HR (95%CI)	P-value	HR (95%CI)	P-value
Age ≥ 60 years	1.25 (0.74–2.11)	0.453		
Male gender	1.16 (0.69–2.05)	0.606		
Child-Pugh ≥ 6	1.01 (0.36–2.84)	0.979		
AFP ≥ 100 ng/ml	1.42 (0.84–2.41)	0.188	1.25 (0.72–2.18)	0.429
PIVKA-II ≥ 100 mAU/ml	1.44 (0.85–2.45)	0.171	1.05 (0.59–1.90)	0.864
Histological grade (poorly)	1.33 (0.60–2.96)	0.485		
Tumor size ≥ 3 cm	1.37 (0.83–2.25)	0.225		
Tumor morphology (multi)	1.09 (0.57–2.06)	0.797		
TNM classification (III, IVa)	1.63 (0.89–2.96)	0.112	1.24 (0.65–2.36)	0.51
Microvascular invasion (Yes)	1.08 (0.65–1.79)	0.765		
HCC recurrence (Yes)	0.73 (0.44–1.23)	0.238		
Nuclear and cytoplasmic hnRNP A2/B1	2.37 (1.33–4.23)	0.004	2.18 (1.19–4.00)	0.012

AFP, α -fetoprotein; HCC, hepatocellular carcinoma.

inhibitors, no telomere shortening of Hsp90 inhibitor-treated cells was observed (data not shown). The present study also demonstrated that the suppression of hnRNP A2/B1 by siRNA inhibited telomerase activity *in vitro*. However, unlike Hsp90, the suppression of hnRNP A2/B1 could potentially shorten telomere length and inhibit cell proliferation, although such an hypothesis should be confirmed by further experiments.

To further examine the clinicopathological significance of hnRNP A2/B1, immunohistochemical staining in clinical HCC samples was performed. Both nuclear and cytoplasmic expression of hnRNP A2/B1 in HCC was significantly related to tumor differentiation and microvascular invasion of HCC (Table 2). Furthermore survival analysis showed a significant correlation between the high nuclear and cytoplasmic expression of hnRNP A2/B1 in HCC and the low survival rate of patients (Table 3, Fig. 6). Although high nuclear and cytoplasmic expression of hnRNP A2/B1 in HCC was not associated with the recurrence rate of HCC (Tables 2, 3), it was associated with the recurrence pattern of HCC. Tumor morphology (multiple HCCs; $P = 0.100$) and vascular invasion ($P = 0.070$) in recurrence was observed more frequently in patients with nuclear and cytoplasmic hnRNP A2/B1-positive HCC than in those with nuclear hnRNP A2/B1-positive HCC, although the difference was not statistically significant (data not shown). The metastatic and invasive features of HCC with nuclear and cytoplasmic expression of hnRNP A2/B1 may contribute to the poor prognosis of affected patients.

Because hnRNP A2/B1 is a RNA shuttling factor(34), nuclear and cytoplasmic expression patterns might reflect increased hnRNP A2/B1 in cells; however, the expression of hTERT is presumably increased and colocalized with hnRNP A2/B1. It was reported that nucleolin, a molecule shuttling into and out of the nucleus, mediates hTERT and localization of hTERT shifted from the nucleus to the cytoplasm depending on its sub-localization(35). Increased hTERT might be associated with tumor differentiation, microvascular invasion and survival of HCC.

While preparing this study, Cui H. *et al.*(36) reported similar findings. They showed increased localization of hnRNP A2/B1 in the cytoplasm of HCC cells during dedifferentiation of HCC. Our study, however, showed the functional relevance of hnRNP A2/B1 on telomerase activity and demonstrated the clinical importance of hnRNP A2/B1 for patient survival.

In conclusion, employing a proteomic screening and molecular biology verification approach revealed a potential HCC biomarker, hnRNP A2/B1, and confirmed its usefulness in the diagnosis of and prediction of prognosis of HCC. Although the present data suggest that hnRNP A2/B1 is clinically significant, the understanding of its underlying mechanisms falls short of that required for the development of practical applications. Further approaches are thus needed to improve the

diagnostic performance of hnRNP A2/B1 for biological and clinical detection of HCC.

Acknowledgements

We thank M. Baba, N. Nishiyama, and Y. Fujita for their technical assistance, and Drs. Y Hinoue, S Aoyama, and K Minouchi at Toyama City Hospital for their help with clinical support.

References

1. Thorgerirsson SS, Grisham JW. Molecular pathogenesis of human hepatocellular carcinoma. *Nat Genet* 2002; **31**: 339–46.
2. Parkin DM, Bray F, Ferlay J, Pisani P. Global cancer statistics. *CA Cancer J Clin* 2005; **55**: 74–108.
3. de Lange T. Ending up with right partner. *Nature* 1998; **392**: 753–54.
4. Blackburn EH. Telomere states and cell fates. *Nature* 2000; **408**: 53–6.
5. Bodnar AG, Ouellette M, Frolkis M, *et al.* Extension of life-span by introduction of telomerase into normal human cells. *Science* 1998; **279**: 349–52.
6. Feng J, Funk WD, Wang SS, *et al.* The RNA component of human telomerase. *Science* 1995; **269**: 1236–41.
7. Weinrich SL, Pruzan R, Ma L, *et al.* Reconstitution of human telomerase with the template RNA component hTR and the catalytic protein subunit hTERT. *Nat Genet* 1997; **17**: 498–502.
8. de Lange T. Protection of mammalian telomerase. *Oncogene* 2002; **21**: 532–40.
9. Yan P, Benhattar J, Seelentag W, Stehle JC, Bosman FT. Immunohistochemical localization of hTERT protein in human tissues. *Histochem Cell Biol* 2004; **121**: 391–7.
10. Desmet VJ, Gerber M, Hoofnagle JH, Manns M, Scheuer PJ. Classification of chronic hepatitis: diagnosis, grading and staging. *Hepatology* 1994; **19**: 1513–20.
11. Shirota Y, Kaneko S, Honda M, Kawai FH, Kobayashi K. Identification of differentially expressed genes in hepatocellular carcinoma with cDNA microarrays. *Hepatology* 2001; **33**: 832–40.
12. Mizuno H, Khurts S, Seki T, *et al.* Human telomerase exists in two distinct active complexes *In Vivo*. *J Biochem* 2007; **141**: 641–52.
13. Masutomi K, Yu EY, Khurts S, *et al.* Telomerase maintains telomere structure in normal human cells. *Cell* 2003; **114**: 241–53.
14. Kim SY, Lee PY, Shin HJ, *et al.* Proteomic analysis of liver tissue from HBx-transgenic mice at early stages of hepatocarcinogenesis. *Proteomic* 2009; **22**: 5056–66.
15. Sun W, Xing B, Sun Y, *et al.* Proteomic analysis of hepatocellular carcinoma by two-dimensional difference gel electrophoresis. *Mol Cell Proteomics* 2007; **6**: 1798–808.
16. Mohammad HS, Kurikihchi K, Yoneyama H, *et al.* Annexin A2 expression and phosphorylation are up-regulated in hepatocellular carcinoma. *Int J Oncol* 2008; **33**: 1157–63.
17. Liang CRM, Leow CK, Neo JCH, *et al.* Proteomic analysis of human hepatocellular carcinoma tissues by two-dimensional difference gel electrophoresis and mass spectrometry. *Proteomics* 2005; **5**: 2258–71.

18. Na K, Lee EY, Lee HJ, *et al.* Human plasma carboxylesterase 1, a novel serologic biomarker candidate for hepatocellular carcinoma. *Proteomics* 2009; **9**: 3989–99.
19. Goldenberg D, Ayesh S, Schneider T, *et al.* Analysis of differentially expressed genes in hepatocellular carcinoma. *Mol Carcinog* 2002; **33**: 113–24.
20. Yokoyama Y, Kuramitsu Y, Takashima M, *et al.* Proteomic profiling of proteins decreased in hepatocellular carcinoma from patients infected with hepatitis C virus. *Proteomics* 2004; **4**: 2111–6.
21. Zhou J, Mulshine JL, Unsworth EJ, *et al.* Purification and characterization of a protein that permits early detection of lung cancer Identification of heterogeneous nuclear ribonucleoprotein-A2/B1 as the antigen for monoclonal antibody 703D4. *J Biol Chem* 1996; **271**: 10760–6.
22. Jing GJ, Xu DH, Shi SL, *et al.* Aberrant expression and localization of hnRNP-A2/B1 is a common event in human gastric adenocarcinoma. *J Gastroenterol Hepatol* 2011; **26**: 108–15.
23. Marrero JA. Screening tests for hepatocellular carcinoma. *Clin Liver Dis* 2005; **9**: 235–51.
24. Celis JE, Gromov P. Proteomics in translational cancer research: toward an integrated approach. *Cancer Cell* 2003; **3**: 9–15.
25. Kawada N. Cancer serum proteomics in gastroenterology. *Gastroenterology* 2006; **130**: 1917–19.
26. Mayeda A, Munroe S, Caveres J, Krainer A. Function of conserved domains of hnRNP A1 and other hnRNP A/B proteins. *EMBO J* 1994; **13**: 5483–95.
27. Abdul-Manan N, Williams K. hnRNP A1 binds promiscuously to oligoribonucleotides: utilization of random and homo-oligonucleotides to discriminate sequence from base-specific binding. *Nucleic Acids Res* 1996; **24**: 4063–70.
28. Munro TP, Magee RJ, Kidd GJ, *et al.* Mutational analysis of a heterogeneous nuclear ribonucleoprotein A2 response element for RNA trafficking. *J Biol Chem* 1999; **274**: 34389–95.
29. Hamilton BJ, Nagy E, Malterg JS, Arrick BA, Rigby WFC. Association of heterogeneous nuclear ribonucleoprotein A1 and C proteins with reiterated AUUUA sequences. *J Biol Chem* 1993; **268**: 8881–7.
30. Hamilton BJ, Burns CM, Nichols RC, Rigby WFC. Modulation of AUUUA response element binding by heterogeneous nuclear ribonucleoprotein A1 in human T lymphocytes. *J Biol Chem* 1997; **274**: 34389–95.
31. Kim MJ, Lyndal W, Derek DK, *et al.* hnRNP A2, a potential ssDNA/RNA molecular adapter at the telomere. *Nucleic Acids Res* 2005; **33**: 486–96.
32. Kamma H, Fujimoto M, Fujiwara M, *et al.* Interaction of hnRNP A2/B1 isoforms with telomeric ssDNA and the *in Vitro* function. *Biochem Biophys Res Commun* 2001; **280**: 625–30.
33. Holt SE, Aisner DL, Baur J, *et al.* Functional requirement of p23 and Hsp90 in telomerase complexes. *Genes Dev* 1999; **13**: 817–26.
34. Nakielny S, Dreyfuss G. Nuclear export of proteins and RNAs. *Curr Opin Cell Biol* 1997; **9**: 420–29.
35. Khurts S, Masutomi K, Delgermaa L, *et al.* Nucleolin interacts with telomerase. *J Biol Chem* 2004; **279**: 51508–15.
36. Cui H, Wu F, Sun Y, Fan G, Wang Q. Up-regulation and subcellular localization of hnRNP A2/B1 in the development of hepatocellular carcinoma. *BMC cancer* 2010; **10**: 356–69.

201324028B (別刷 5/6)

厚生労働科学研究費補助金 難治性疾患等克服研究事業

(難治性疾患克服研究事業)

難治性の肝・胆道疾患に関する調査研究

平成23～25年度 総合研究報告書

研究成果の刊行物・別刷 (平成25年度)

分冊 6 - 5

研究代表者 坪内 博仁

平成26 (2014) 年 3 月

V. 研究成果の刊行物・別刷
(平成25年度)

分冊 6 - 5